Identifying State-dependent Modulations In Functional Connectivity: A Group Theoretic Baseline-Correction

Kyle J. Curham, John J. B. Allen
Department of Psychology - University of Arizona - Tucson, Arizona

Introduction

- Functional connectivity (FC) is defined as the statistical interdependence between regions of interest (ROIs).
- Spatiotemporal FC patterns can change dynamically within the constraints of a fixed anatomical structure.
  - **The averaged spatial pattern over time of FC may not resemble *any* of the configurations that occur transiently within the scanning period** [1]**.**
- Geodesic regression is a new method to look at time-resolved FC that allows us to:
  - smoothly interpolate between arbitrary starting and ending FC configurations, and
  - study higher-order aspects of variability, such as the rate at which coherence and phase synchronization are modulated.
- Baseline-correction for FC matrices:
  - FC dynamics may appear manifestly different, but those **differences could be explained by differences in the initial conditions.**
- The current study investigated theta-band FC dynamics in EEG time-series on a forced-choice speeded-response flanker task.
  - A novel statistical test is used to detect correct/incorrect response differences in FC dynamics, independent of baseline FC.

Model

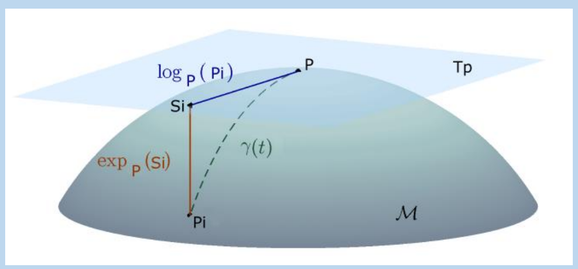

Figure 1: The group of positive-definite (HPD) covariance matrices forms a smooth and continuous manifold [2].

- The matrix exponential is the generating function for the group of HPD matrices.
  - Given any Hermitian matrix A, there is a unique corresponding positive-definite matrix e^{A}, and inverse matrix e^{-A}.
- Infinitesimal transformations from one position to the next can be integrated over time, yielding a geodesic parameterized by t, e^{tA}.
  - The set of geodesics emanating from the identity element at t=0 represents the set of all possible solutions to linear dynamical systems of the form:

$$\dot{X} = AX$$
$$X(t) = e^{tA}X(0)$$

- In general, geodesics may emanate from any point on the HPD manifold.
  - Given a tangent vector V and base-point P, an integral curve can be generated.
- Baseline-correction:
  - The HPD manifold is not closed under subtraction; the difference between two HPD matrices may not be HPD.
  - Solution: transport tangent vector to identity at each time-point.
    - There is an equivalence class on the manifold, such that multiple vectors emanating from different points map onto the same vector emanating from identity [3].
      - represents the predicted change in FC, relative to baseline FC.
    - Parallel Transport: defined with respect to an affine connection between tangent spaces, such that moving V along its associated geodesic maps tangent vectors into one another:

$$\Gamma_{s\to t}V(s) = V(t)$$

- An invariant distance measure can be defined by transporting V to identity and computing the matrix inner-product with itself [4]:

$$\langle V|V\rangle_P = Tr\left(P^{-1/2}VP^{-1}VP^{-1/2}\right)$$

- Geodesic regression minimizes the sum-of-squared geodesic distances between sample covariance matrices and their predicted position on the geodesic [5].
  - The output yields the best-fit solutions for P and V.

Results

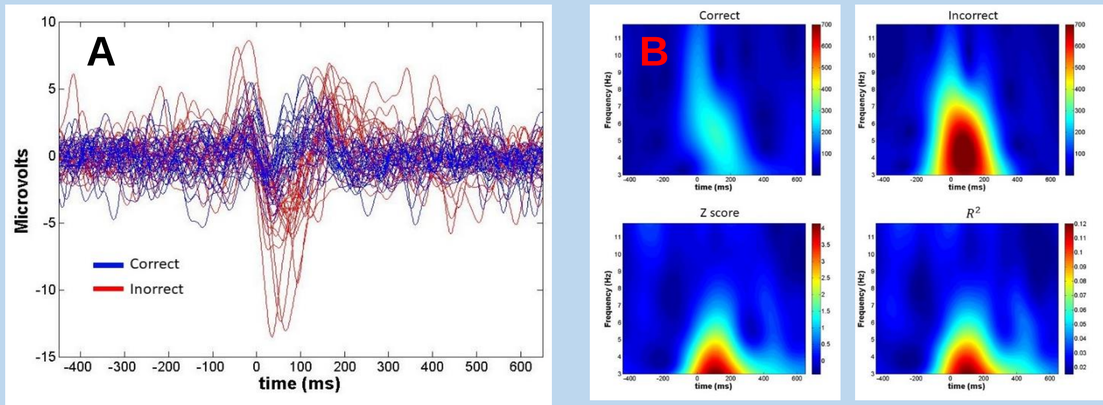

Figure 2: A) A significant fronto-central error-related negativity (ERN) was detected in 27/30 participants. B) There was significantly more fronto-central theta coherence in 21/30 participants following incorrect trials, compared to correct trials.

Figure 3: The average R^2 for geodesic regression algorithm on single-trial EEG was 0.765 (right):

$$R^2 = 1 - \frac{\sum_{i=1}^{N}\delta(y,y_i)^2}{\sum_{i=1}^{N}\delta(\bar{y},y_i)^2}$$

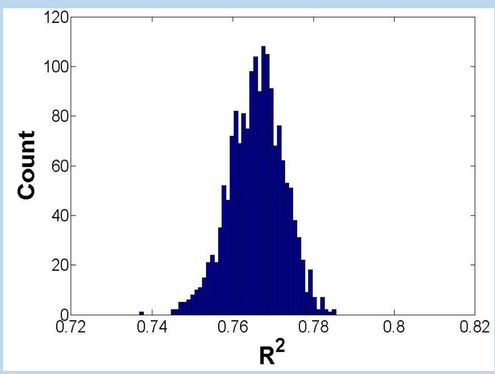

- **Does FC differ between correct/incorrect trials?**
  - Null hypothesis: length of the geodesic connecting the condition means is not significantly greater than zero.

Figure 4: A) FC differed between correct/incorrect trials in 21/30 participants. B) FC differences correlated with ERN Z score (r = 0.714).

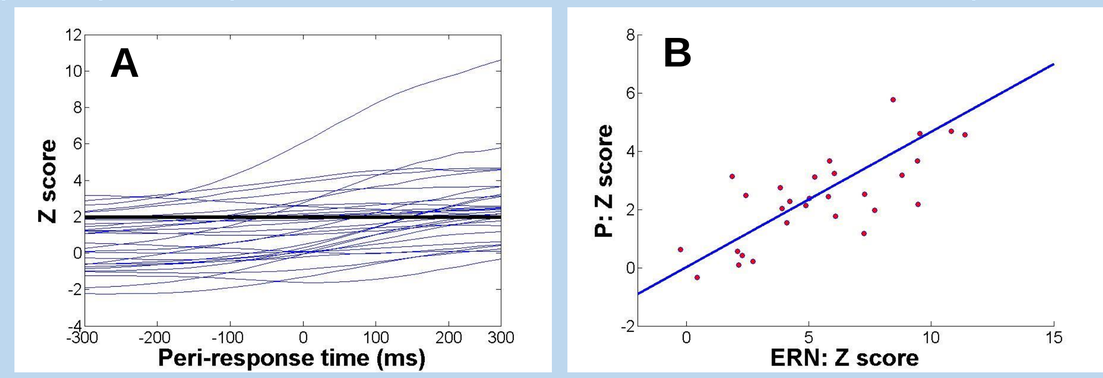

- **Does FC dynamics differ between correct/ incorrect trials?**
  - Null hypothesis: mean tangent vectors belong to the same equivalence class.

Figure 5: A) FC dynamics differed between correct/incorrect trials in 14/30 participants (below). B) FC dynamics were correlated with ERN Z score (r = 0.582).

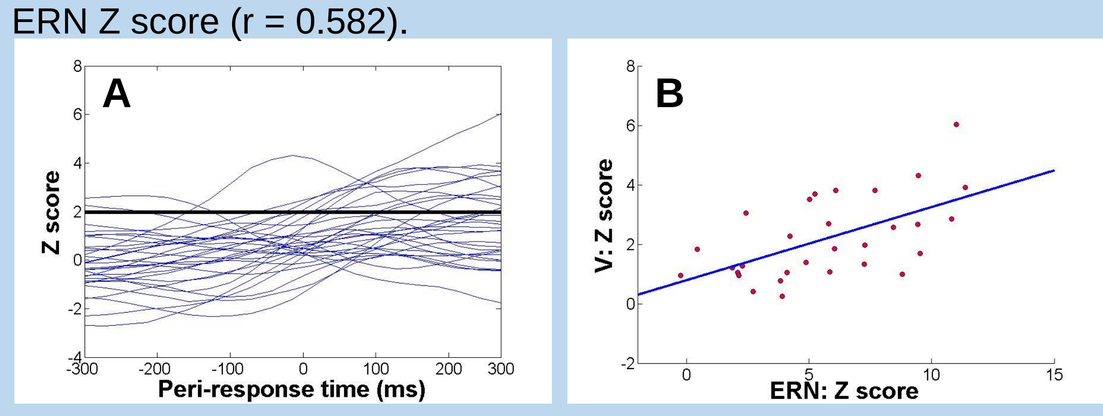

Conclusions

- The current study provides:
  - strong evidence for dynamic FC in single-trial EEG time-series;
  - evidence that FC dynamics differs between incorrect and correct responses on a forced-choice speeded-response task.
    - Independent of baseline differences in FC.
    - Low hit rate could be due to sensitivity to window width or montage choices.

References

Hutchison, R. M., Womelsdorf, T., Allen, E. A., Bandettini, P. A., Calhoun, V. D., Corbetta, M., … Chang, C. (2013). NeuroImage Dynamic functional connectivity : Promise , issues , and interpretations. *NeuroImage*, *80*, 360–378.

Barachant, A., Bonnet, S., Congedo, M., & Jutten, C. (2010). Riemannian geometry applied to BCI classification. *Lecture Notes in Computer Science (Including Subseries Lecture Notes in Artificial Intelligence and Lecture Notes in Bioinformatics)*, *6365 LNCS*, 629–636.

Sengupta, B., Tozzi, A., Cooray, G. K., Douglas, P. K., & Friston, K. J. (2016). Towards a Neuronal Gauge Theory. *PLoS Biology*, *14*(3), 1–12.

Pennec, X., Fillard, P., & Ayache, N. (2005). A Riemannian Framework for Tensor Computing.

Fletcher, P. T. (2013). Geodesic Regression on Riemannian Manifolds. *International Journal of Computer Vision*, *105*(2), 171–185.

Reprints available at: http://jallen.faculty.arizona.edu/content/conference-presentations

Introduction

Measures such as phase synchronization and coherence have been used to infer functional relationships in EEG time-series, but they suffer from serious limitations posed by non-stationary confounds (Zalesky & Breakspear, 2015; Zhan & Halliday, 2005). **In general, parameters may change continuously over the estimation interval.** However, these measures require many samples, extending over large epochs. Matrices must be estimated from short windows such that the change in parameters is negligible over the interval, balanced by the need for enough samples to get valid estimates.

The approach considered in this report **explicitly models non-stationary functional connectivity by fitting a regression line in the space of functional configurations**, to smoothly interpolate between arbitrary starting and ending configurations. This method generalizes linear regression to multi-dimensional curved manifolds, representing the shortest possible path between configurations (Fletcher, 2013). This approach is fully multivariate, controlling for multiple comparisons. Moreover, **this framework allows for a novel baseline-correction that yields the predicted change in functional connectivity relative to the initial configuration.** This report includes algorithms to fit the geodesic regression model for single-trial EEG epochs, characterize the quality of model fit, and compute the geometric mean of models across trials. Differences between conditions are assessed via a novel non-parametric permutation omnibus test at the subject level. Critically, **this test can reveal differences in functional connectivity dynamics, independent of baseline functional connectivity.**

This approach can be applied across research domains and imaging modalities, but the current investigation focuses on functional connectivity as measured by EEG during a forced-choice speeded-response task. During the task, participants respond with a button press to centrally presented letter stimuli, while ignoring flanking letters to the left and right of the target (figure 1).

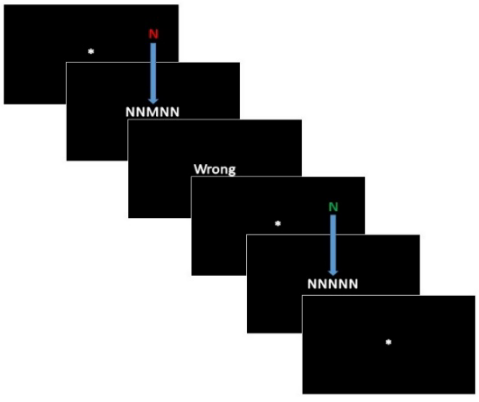

Figure 1: Participants completed a modified Eriksen Flankers task (Eriksen and Eriksen, 1974; Eriksen and Schultz, 1979). They were asked to press one of two response buttons using their thumbs to identify the center letter in a string that is either congruent (e.g., MMMMM; 200 trials) or incongruent (e.g., NNMNN; 200 trials) with the flanking stimuli. Participants should be more likely to make an error when the central letter is incongruent with the flanking stimuli. Ten blocks tested different pairs of letters and their reversals, 20 trials each, for a total of 400 trials. Target-hand mappings were reversed after each block to increase response conflict. Stimuli were presented for 200 ms, and the flanking stimuli were presented 33 ms prior to the target, with an SOA of 100 ms. The basic trial sequence is depicted (left). Post-response connectivity is examined between response-onset and feedback presentation.

Geodesic Regression

Geodesic regression amounts to finding the best-fit solution that minimizes the sum-of-squared geodesic distances between the sample covariance matrices and their predicted position on the

geodesic. In this report, the geodesic regression algorithm is initialized with a zero length tangent vector emanating from the geometric mean of all the samples. Sample covariance matrices are initially estimated on the interval [-450,-300] preceding the response. This window is shifted in 13 equally spaced, 150 ms steps to generate the set of covariance matrices to be entered into the geodesic regression algorithm. Every matrix is associated with a particular point on the geodesic, obtained by scaling t such that it lies on the interval 0 to 1, over the length of the geodesic segment. The model definition is given by (Fletcher, 2013):

$$y = Exp(Exp(P, t_i V), \epsilon)$$

where ϵ is the residual vector, and $Exp(P, t_i V)$ is the predicted covariance on the geodesic when t = t_i. Guesses for P and V are modified iteratively, until the sum-of-squared geodesic distances is minimized. The solution is given by minimizing the objective function:

$$\underset{(P,V)}{argmin}\ O = \frac{1}{2}\sum_{i=1}^{N} \langle \mathrm{Log}(Exp(P, t_i V), y_i) | \mathrm{Log}(Exp(P, t_i V), y_i) \rangle_P$$

For demonstration, samples were drawn from a bivariate normal distribution with unit variances, and transformed such that they lie on the surface of a 2-torus. A final and ending configuration were chosen at random, and a geodesic was generated, interpolating between them (figure 3).

Figure 3: Geodesic regression on a torus. A 2-torus undergoes continuous deformations and rotations as the covariance changes along the geodesic. The geodesic was segmented into 100 time-steps, with a sample covariance matrix for each time-step. Each matrix was estimated from 3000 samples. The resulting 2x2 HPD matrices were entered into the geodesic regression algorithm (R^2=.9991).

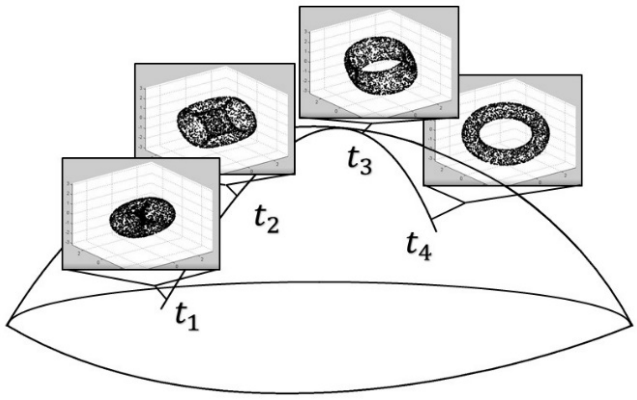

Baseline Correction

Baseline functional connectivity is likely to be non-zero in most participants, on most trials. Even in the absence of task or instructions, participants experience general arousal in the novel experimental environment, and resting-state dynamics are intrinsically non-stationary. Moreover, during engaging tasks where participants have to exercise cognitive control across domains, such as perceptual discrimination and motor preparation, participants may exhibit anticipatory changes in functional connectivity.

Functional connectivity dynamics may look very different, but those differences may be explained by differences in the initial conditions. There is an equivalence class on the manifold, such that multiple vectors emanating from different points map onto the same vector emanating from the identity element,

under the parallel transport (Sengupta, Tozzi, Cooray, Douglas, & Friston, 2016). The relationship between these models is described by an isometric (distance-preserving) coordinate transformation on the HPD manifold. The proposed baseline-correction yields the predicted change in covariance, relative to the base point. On each trial, V is transported to the identity element: $\mathrm{P}^{-1/2}\mathrm{V}\mathrm{P}^{-1/2}$.

Permutation Significance Testing

Regression Model

The significance of the geodesic regression model can be evaluated using robust permutation statistics. Under the null hypothesis, the length of the geodesic is zero, and the base point is equal to the geometric mean of all the samples ($\overline{y}$). Therefore, the samples are exchangeable under the null hypothesis. Geodesic regression is performed over several hundred permutation, shuffling the condition labels on each iteration. The R^2 is given by the ratio of the sum-of-squared geodesic distances between the predicted and observed covariance matrices, and the sum-of-squared distances to the geometric mean of all the samples:

$$R^2 = 1 - \frac{\sum_{i=1}^{N}\langle \mathrm{Log}(Exp(P, t_i V), y_i) | \mathrm{Log}(Exp(P, t_i V), y_i)\rangle_P}{\sum_{i=1}^{N}\langle \mathrm{Log}(\overline{y}, y_i) | \mathrm{Log}(\overline{y}, y_i)\rangle_P}$$

Over several hundred permutations, the distribution of the expected R^2 under the null hypothesis is constructed. Each R^2 value is Fischer-Z transformed. The non-parametric construction of the null distribution admits a robust significance test by simply counting the number of permutations with an R^2 value exceeding the true R^2. If the fraction of permutations that exceeds the true R^2 is not larger than threshold, a statistically significant effect can be inferred.

Omnibus Test on the Manifold

An omnibus test can be constructed on the manifold to evaluate whether the geodesic distance between conditions is significantly greater than zero. Such a test would indicate whether or not functional connectivity is statistically significantly different between conditions, but it does not indicate where the differences occur. Under the null hypothesis, the length of the geodesic connecting the mean of each condition is zero, and the base point is equal to the geometric mean of all the samples. This test is equivalent to geodesic regression with dummy coding, such that all samples are at the endpoints of the geodesic. Since the group labels are exchangeable, robust permutation statistics can be performed as before. After several hundred permutations, the true R^2 is compared with the distribution of R^2 under the null hypothesis.

Omnibus Test on the Tangent Bundle

Differences in functional connectivity dynamics, between conditions, can be assessed with a significance test on the tangent bundle. The algorithm is initialized by transporting each tangent vector to identity. Following the baseline-correction procedure, vectors all lie in the same linear tangent space, so they can be directly compared. The mean tangent vector is computed for each condition, v1 and v2.

Under the null hypothesis, $\|v_1 - v_2\| = 0$, so the condition labels are exchangeable and permutation testing can be performed.

Data Collection, Preprocessing and Analysis

Sample Description

Thirty medically healthy young adults age 18-23 were recruited from the University of Arizona subject pool in exchange for course credit. All participants reported they were free from past neurological trauma and psychopathology as delineated in the Diagnostic and Statistical Manual (DSM), 5th edition, had normal or corrected-to-normal vision, and were free from current psychoactive medication use.

EEG Data Collection

EEG was recorded from 64 scalp electrode sites using Synamps2 amplifiers (bandpass 0.05 to 100 Hz) at a 1,000 Hz sampling rate using a stretch Ag-AgCl electrode cap, with impedances < 15 kΩ. Sensors were placed using adhesive collars above and below the left eye to measure ocular movement, on the side of the eyes, and behind each ear to allow for electronic referencing. At the locations of these facial sensors, skin was prepped using Omni-prep and an alcohol wipe. All sites were grounded anterior to Fz and referenced online posterior to Cz.

EEG Preprocessing

All files were screened by hand to ensure fidelity, removing any residual and EMG artifacts. A 3 Hz digital highpass FIR filter is applied in post-processing. The Gratton method was used for ocular artifact correction (Gratton, Coles, & Donchin, 1983). All participants had EEG data for at least 10 epochs for each condition (correct, incorrect). Generally, participants responded correctly far more often than they respond incorrectly. To control for differences in trial count, correct and incorrect trials were match for reaction time in equal numbers. For example, if there were 25 incorrect responses, then 25 correct responses with the most similar reaction times were chosen for comparison. All EEG epochs were re-referenced offline to the average reference. After re-referencing, the scalp channel montage was down-sampled to 18 electrodes to reduce computational run-time (figure 4). Trials were epoched [-1500 2000] ms peri-stimulus. Such a long window was used to accommodate edge artifacts from the wavelet convolution.

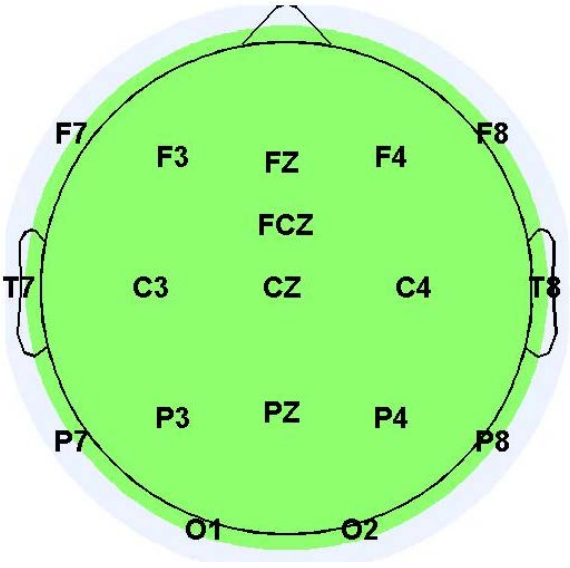

Figure 4: Scalp electrode positions

Time–frequency calculations were computed using custom-written Matlab (The MathWorks) routines based on (M. X. Cohen, 2014). The EEG time-series for each epoch were convolved with a set of

complex Morlet wavelets, defined as a Gaussian-windowed complex sinusoid: $e^{2i\pi ft}e^{-t^2/2\sigma^2}$ where t is time, f is frequency (which increased from 3 to 50 Hz in 40 logarithmically spaced steps), and σ defines the width of each frequency band, in cycles, set according to 4.5/(2πf) (Trujillo and Allen, 2007). The result of the convolution is a similarity measure between the EEG signal and complex sinusoids. The instantaneous phase at each electrode can be estimated from the resulting analytic signal:

$$\theta = arctan(Real(s)^2/Imag(s)^2)$$

Where s is the complex signal at a given time. Each epoch was then cut into a smaller epoch containing data 300 ms prior to and following the response, for a total of 600 ms on each trial.

References

Cavanagh, J. F., Cohen, M. X., & Allen, J. J. B. (2009). Prelude to and resolution of an error: EEG phase synchrony reveals cognitive control dynamics during action monitoring. *The Journal of Neuroscience : The Official Journal of the Society for Neuroscience*, *29*(1), 98–105. http://doi.org/10.1523/JNEUROSCI.4137-08.2009

Cohen, M. X. (2017). Multivariate cross-frequency coupling via generalized eigendecomposition, 1–26. http://doi.org/10.7554/eLife.21792

Cohen, X. M. (2014). *Analyzing Neural Time Series Data*. *MIT Press*. http://doi.org/10.1007/s13398-014-0173-7.2

Fletcher, P. T. (2013). Geodesic Regression on Riemannian Manifolds. *International Journal of Computer Vision*, *105*(2), 171–185. http://doi.org/10.1007/s11263-012-0591-y

Gratton, G., Coles, M. G. H., & Donchin, E. (1983). A new method for off-line removal of ocular artifact. *Electroencephalography and Clinical Neurophysiology*, *55*(4), 468–484. http://doi.org/10.1016/0013-4694(83)90135-9

Kim, H. J., Bendlin, B. B., Adluru, N., Collins, M. D., Chung, M. K., Johnson, S. C., … Singh, V. (2014). Multivariate General Linear Models (MGLM) on Riemannian Manifolds with Applications to Statistical Analysis of Diffusion Weighted Images. http://doi.org/10.1109/CVPR.2014.352

Pennec, X., Fillard, P., & Ayache, N. (2005). A Riemannian Framework for Tensor Computing.

Sengupta, B., Tozzi, A., Cooray, G. K., Douglas, P. K., & Friston, K. J. (2016). Towards a Neuronal Gauge Theory. *PLoS Biology*, *14*(3), 1–12. http://doi.org/10.1371/journal.pbio.1002400

Sra, S., & Hosseini, R. (2015). Conic geometric optimization on the manifold of positive definite matrices. *SIAM Journal on Optimization*, *25*(1), 713–739. http://doi.org/10.1137/140978168

Trujillo, L. T., & Allen, J. J. B. (2007). Theta EEG dynamics of the error-related negativity. *Clinical Neurophysiology*, *118*(3), 645–668. http://doi.org/10.1016/j.clinph.2006.11.009

Zalesky, A., & Breakspear, M. (2015). NeuroImage Towards a statistical test for functional connectivity dynamics. *NeuroImage*, *114*, 466–470. http://doi.org/10.1016/j.neuroimage.2015.03.047

Zhan, Y., & Halliday, D. (2005). Detecting the time-dependent coherence between non-stationary electrophysiological signals – A combined statistical and time-frequency approach Charing Cross Hospital & Division of Neuroscience and Mental Health, 1–33.